COMMENTARY

John S. Olson · George N. Phillips, Jr.

Myoglobin discriminates between O_2, NO, and CO by electrostatic interactions with the bound ligand

Abstract Most biological substrates have distinctive sizes, shapes, and charge distributions which can be recognized specifically by proteins. In contrast, myoglobin must discriminate between the diatomic gases O_2, CO, and NO which are apolar and virtually the same size. Selectivity occurs at the level of the covalent Fe-ligand complexes, which exhibit markedly different bond strengths and electrostatic properties. By pulling a water molecule into the distal pocket, His64(E7)[1] inhibits the binding of all three ligands by a factor of ~ 10 compared to that observed for protoheme-imidazole complexes in organic solvents. In the case of O_2 binding, this unfavorable effect is overcome by the formation of a strong hydrogen bond between His64(E7) and the highly polar FeO_2 complex. This favorable electrostatic interaction stabilizes the bound O_2 by a factor of ~ 1000, and the net result is a 100-fold increase in overall affinity compared to model hemes or mutants with an apolar residue at position 64. Electrostatic interaction between FeCO and His64 is very weak, resulting in only a two- to three-fold stabilization of the bound state. In this case, the inhibitory effect of distal pocket water dominates, and a net fivefold reduction in K_{CO} is observed for the wild-type protein compared to mutants with an apolar residue at position 64. Bound NO is stabilized $\sim$ tenfold by hydrogen bonding to His64. This favorable interaction with FeNO exactly compensates for the tenfold inhibition due to the presence of distal pocket water, and the net result is little change in K_{NO} when the distal histidine is replaced with apolar residues. Thus, it is the polarity of His64 which allows discrimination between the diatomic gases. Direct steric hindrance by this residue plays a minor role as judged by: (1) the independence of K_{O_2}, K_{CO}, and K_{NO} on the size of apolar residues inserted at position 64, and (2) the observation of small decreases, not increases, in CO affinity when the mobility of the His64 side chain is increased. Val68(E11) does appear to hinder selectively the binding of CO. However, the extent is no more than a factor of 2–5, and much smaller than electrostatic stabilization of bound O_2 by the distal histidine.

Introduction

Mammalian myoglobin functions as a storage protein in striated muscle to provide a continuous supply of O_2 to the terminal mitochondrial oxidase. During relaxation, red blood cells circulating through capillary beds provide O_2 for both oxidative phosphorylation and oxygenation of myoglobin. During contraction no blood flow occurs, and oxygen is supplied to the mitochondria by release from myoglobin. In order to perform this storage-delivery function, myoglobin has evolved a relatively high affinity for O_2. It has a P_{50}[2] value of $\sim 1 \, \mu M$, which is intermediate between that of hemoglobin in red cells ($P_{50} \sim 20$–$30 \, \mu M$) and the K_M of cy-

J. S. Olson (✉) · G. N. Phillips, Jr
Department of Biochemistry and Cell Biology
and the W. M. Keck Center for Computational Biology,
Rice University MS 140, 6100 Main,
Houston, TX 77005-1892, USA
Tel.: 1-713-527-4762; Fax: 1-713-285-5154;
e-mail: olson@bioc.rice.edu

---

[1] The alphanumeric code listed in parentheses after the sequence number (e.g. E7, E11, B10) refers to the position of the residue within the helices and loops of the myoglobin folding pattern. For example, E7 refers to the seventh residue in the E-helix. The recombinant myoglobins contain an "extra" N-terminal Met to allow expression in *Escherichia coli*. This residue is numbered "0" to keep the sequence numbers of the remaining amino acids the same as that in the native protein

[2] P_{50} is rigorously defined as the partial pressure of dioxygen required to obtain 50% saturation of the iron sites in the protein. We use the term here to represent the dissolved concentration of free O_2 required to obtain 50% binding. In the case of myoglobin, P_{50} equals the equilibrium dissociation constant, since only a single binding process occurs

Table 1 O_2, NO, and CO equilibrium association constants and O_2 dissociation rate constants for wild-type and mutant sperm whale myoglobins and chelated protoheme at pH 7, 20 °C

Protein or model heme	K_{O_2} (μM^{-1})	k_{O_2} (s^{-1})	K_{CO} (μM^{-1})	K_{NO} (μM^{-1})
A. Wild-type or native SW Mb	1.1	15	27	220 000
B. Chelated protoheme [a] in:				
Benzene	0.015	4200	330	n.d.
2% soap micelles	0.55	47	300	n.d.
C. Apolar His(E7) mutants of recombinant SW Mb				
H64Q	0.18	130	82	320 000
H64G	0.090	1700	150	280 000
H64A	0.023	2300	69	130 000
H64V	0.011	10 000	150	250 000
H64I	0.014	6400	170	190 000
H64L	0.022	5400	1100	1 500 000
H64F	0.0075	10 000	83	180 000
D. Mutants that enhance rotation of His(E7) but retain water				
F46A	0.060	160	6.0	28 000
F46V	0.070	220	17	73 000
E. Mutants that alter hindrance by residue E11				
V68A	1.2	18	56	240 000
V68I	0.22	14	2.1	36 000
F. Mutants that alter distal pocket polarity and water occupancy				
V68T	0.070	39	7.5	12 000
L29F	15	1.4	37	1 300 000

[a] The model heme is protoheme mono-3-(1-imidazoyl)-propylamide monomethyl ester dissolved in either benzene or 2% myristyltrimethylammonium bromide, 0. 1 M sodium phosphate buffer pH 7. The data were taken from Olson et al. [14] and Traylor et al. [11–13]

tochrome oxidase (~ 0.01 μM). Simple protoheme-imidazole complexes in apolar solvents show an affinity for reversible O_2 binding which is a least 100 times smaller than that for myoglobin (Table 1). In addition, these model compounds autooxidize in seconds compared to 1–2 days for oxymyoglobins [1]. Thus the protein portion of myoglobin is conferring substantial increases in both oxygen affinity and resistance to oxidation.

Myoglobin is also able to discriminate in favor of O_2 binding and against CO binding when compared to simple model heme compounds. As shown in Table 1, the ratio of CO to O_2 affinity (K_{CO}/K_{O_2} or *M*-value) is ~ 20000 for chelated protoheme in benzene, whereas that for sperm whale myoglobin is only 25. This discrimination is required to allow myoglobin to function as an oxygen storage protein in the presence of low levels (≤ 1 μM) of CO, which is produced continuously as a result of heme catabolism, neuronal function, and cell signaling in the vasculature [2–4]. In most enzymatic reactions, specificity is a result of the protein recognizing the exact shape and charge distribution of the substrate molecule. In the case of O_2 and CO binding to deoxymyoglobin, selective recognition can only occur after the iron-ligand complex is formed, since both gases are roughly the same size and apolar. The key structural features of the FeO_2 and FeCO complexes in myoglobin are summarized in Fig. 1.

Up until 1988–1990, the most widely accepted view was that steric crowding by amino acid side chains on the distal side of the heme group inhibits CO binding by preventing a linear Fe–C–O geometry [5–8]. The inherently bent Fe–O–O geometry allows a much better "fit" for the bound ligand molecule (Fig. 1). Although seriously challenged by more recent studies, this interpretation is still presented in most undergraduate biochemistry textbooks. The alternative view is that myoglobin preferentially stabilizes bound oxygen by favorable electrostatic interactions with the polar FeO_2 complex in which there is net movement of electron density from the iron atom to the oxygen atoms. Some authors have argued that the complex can be thought of as $Fe(III)^+$-O_2.- where the bound ligand has characteristics of superoxide anion [9, 10]. In contrast, the FeCO complex is apolar and unlikely to interact strongly with polar amino acid side chains. Traylor and coworkers argued that the 50-fold increase in oxygen affinity observed when chelated protoheme is taken from benzene and put into myristyltrimethylammonium micelles is due to stabilization of the partial negative charge on the bound O_2 (Table 1) [11–14]. In this case, the favorable electrostatic interactions are less specific and come from either water bound to the micelles or the quaternary amine. In contrast, the change from an apolar solvent to soap micelles has little effect on CO affinity.

The mechanism of ligand discrimination has been examined systematically over the past 10 years by both site-directed mutagenesis of recombinant myoglobins and the construction of new model compounds. The synthetic heme work has been reviewed by Momenteau and Reed [10], and we have presented reviews of the mutagenesis studies [15, 16]. Virtually all of these new experiments suggest that ligand discrimination occurs
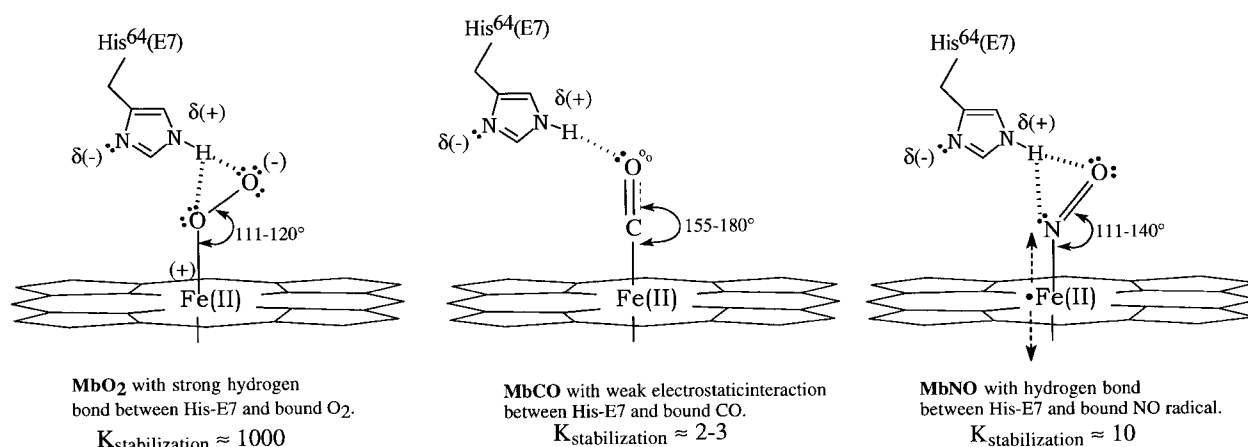
MbO₂ with strong hydrogen bond between His-E7 and bound O_2.
$K_{stabilization} \approx 1000$

MbCO with weak electrostaticinteraction between His-E7 and bound CO.
$K_{stabilization} \approx 2\text{-}3$

MbNO with hydrogen bond between His-E7 and bound NO radical.
$K_{stabilization} \approx 10$

Fig. 1 Proposed structures of Fe(II)O₂, Fe(II)NO, and Fe(II)CO in native sperm whale myoglobin. The resonance structures are based on the stretching frequencies for the O–O (~ 1105 cm^{-1}, order ≈ 1), C–O (~ 1945 cm^{-1}, order ≈ 2.5), and N–O (~ 1625 cm^{-1}, order ≈ 2) bonds. The Fe-ligand stretching frequencies range from ~ 510 (Fe–CO) to 570 cm^{-1} (Fe–O₂) implying an order of ~ 1 for all three complexes [8, 34–42]. The range of bond angles for FeO₂ and FeCO were taken from crystal structures determined by Phillips and coworkers [17, 23, 26, 30, 38, 42, 45]. The range of bond angles for FeNO were taken from the model heme work of Scheidt and coworkers [41] and structures for native and L29F sperm whale MbNO [52][3]. The structure of FeNO in native myoglobin is shown in Fig. 3 compared to that of the CO and O₂ forms of wild-type protein [23]

by electrostatic interactions and that steric hindrance is not a key factor. The following commentary presents a formal mechanistic description of this interpretation. For brevity, we have focused on our own site-directed mutagenesis studies carried out in collaboration with Barry Springer and Stephen Sligar at the University of Illinois, Anthony Wilkinson at York University, and Masao Ikeda-Saito at Case Western Reserve University. More balanced presentations are given in our previous general reviews. We have included new data for the binding of NO which serve as a test of the generality of the electrostatic mechanism.

General mechanism of ligand binding to deoxymyoglobin

Ligand binding to sperm whale myoglobin can be considered in terms of the four reactions shown in Fig. 2. More precise three-dimensional orientations of the key amino acid residues are given in Fig. 3. The first two steps involve movement of the ligand molecule into the protein to form intermediate C, which contains a noncovalently bound ligand in the interior of the heme pocket. This binding requires displacement of a water molecule that is hydrogen bonded to the N atom of the distal histidine (His64) in deoxymyoglobin [17]. Intermolecular binding to the iron atom can also be considered as a two-step process involving formation of the

iron-ligand bond described by K_{bond} and then electrostatic stabilization described by $K_{stabilization}$.

The fractional extent of iron-ligand bond formation, Y, is defined by the ratio $([D]+[E])/([A]+[B]+[C]+[D]+[E])$, where the letters refer to the intermediates shown in Fig. 2. The relative concentrations of the these intermediates are determined by K_{H_2O}, K_{entry}, K_{bond}, $K_{stabilization}$, $[H_2O]$, and $[X]$ where X is the free ligand. If [B] is defined as 1, the relative values of [A], [C], [D], and [E] are $K_{H_2O}[H_2O]$, $K_{entry}[X]$, $K_{bond}K_{entry}[X]$, and $K_{stabilization}K_{bond}K_{entry}[X]$, respectively. These definitions lead to the following general expression for fractional saturation:

$$Y = \frac{\dfrac{K_{entry}K_{bond}(1+K_{stabilization})}{1+K_{H_2O}[H_2O]}[X]}{1+\dfrac{K_{entry}(1+K_{bond}(1+K_{stabilization)})}{1+K_{H_2O}[H_2O]}[X]} \quad (1)$$

For O₂, CO, and NO binding the value of $K_{bond}(1+K_{stabilization})$ is $\gg 1$ (see Table 2), and Eq. 1 reduces to a simple hyperbolic expression with an overall equilibrium constant equal to:

$$K_{overall} = \frac{K_{entry}K_{bond}(1+K_{stabilization})}{1+K_{H_2O}[H_2O]} \quad (2)$$

Equation 2 provides a convenient framework for interpreting the effects of mutagenesis shown in Table 1. First, ligand binding is opposed by the presence of distal pocket water. In terms of Fig. 2, ligand can only react with the fraction of deoxymyoglobin that has an "empty" or anhydrous distal pocket, i.e. $1/(1+K_{H_2O}[H_2O])$. Second, the value of K_{entry} is determined by the free volume in the distal pocket, which is governed by the size of residues 29, 43, 68, and 107 (Fig. 3) [16]. Third, K_{bond} reflects primarily the inherent chemical reactivity of the ligand, but this parameter can be affected by direct steric hindrance of the bound ligand by distal amino acid residues, changes in the volume available to the non-covalently bound ligand, and/or proximal constraints that influence iron reactivity. Fourth, $K_{stabilization}$ reflects the strength of electrostatic

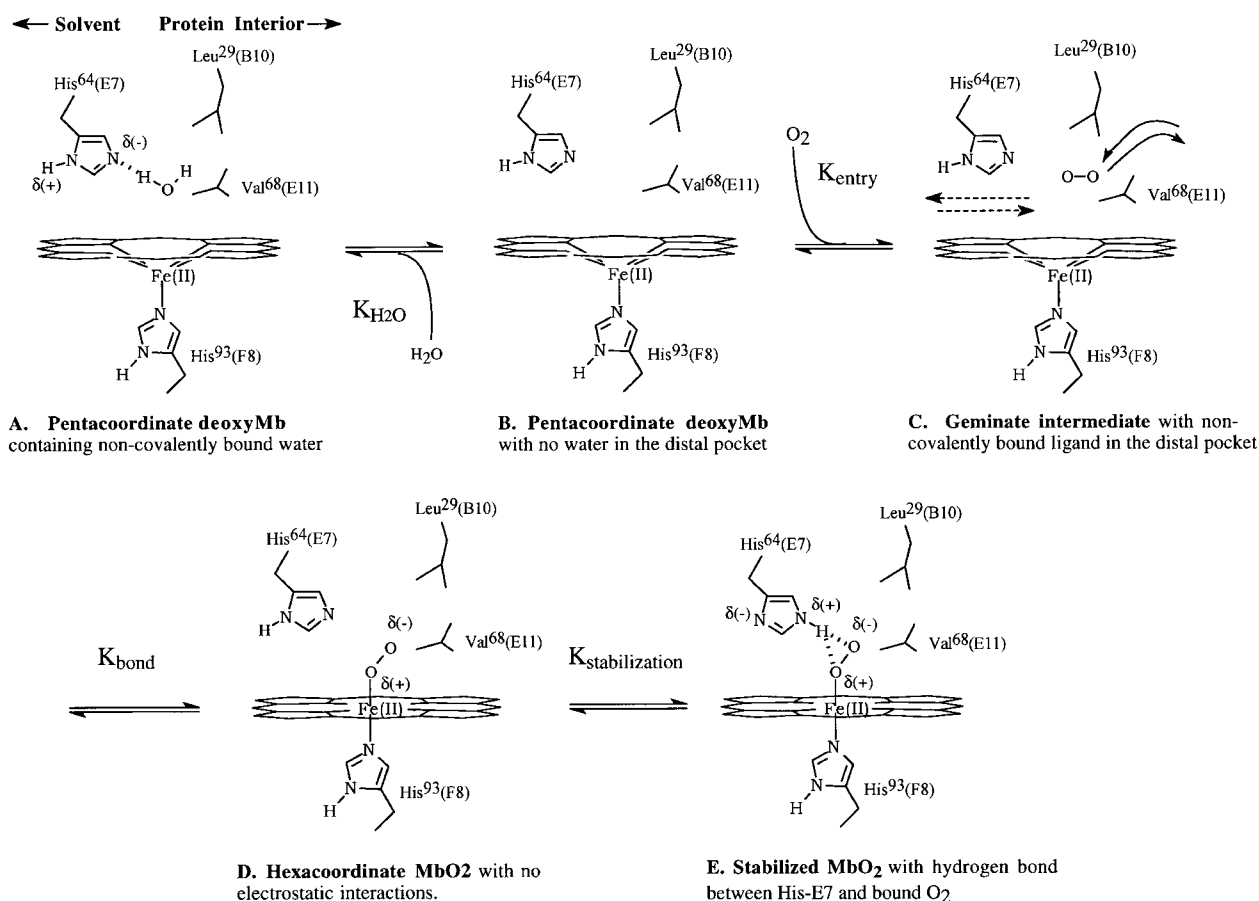← Solvent   Protein Interior →

A. Pentacoordinate deoxyMb
containing non-covalently bound water

B. Pentacoordinate deoxyMb
with no water in the distal pocket

C. Geminate intermediate with non-covalently bound ligand in the distal pocket

D. Hexacoordinate MbO$_2$ with no electrostatic interactions.

E. Stabilized MbO$_2$ with hydrogen bond between His-E7 and bound O$_2$

Fig. 2 Four-step scheme for O$_2$ binding to sperm whale myoglobin

interactions between distal residues and the bound ligand. Thus, the distal histidine inhibits ligand binding indirectly by requiring water displacement and enhances binding directly by stabilization of the bound state. The net effect is determined by the ratio $(1 + K_{\text{stabilization}})/(1 + K_{\text{H}_2\text{O}}[\text{H}_2\text{O}])$, where $K_{\text{stabilization}}$ depends on the exact electrostatic properties of the iron-ligand complex.

Regulation of ligand affinity by His64(E7)

Replacement of the distal histidine with apolar amino acids causes a marked decrease in oxygen affinity. As shown in Table 1, there is no systematic dependence on the size of the apolar residue. The average value of K_{O_2} for 13 different recombinant sperm whale, pig, and human myoglobin mutants with Ala, Val, Ile, Leu, and Phe at the E7 position is 0.01 ± 0.01 μM^{-1} at pH 7, 20° [15]. Quillin et al. [17] have shown that no distal pocket water is present in the crystal structures of Val64 and

Leu64 sperm whale deoxymyoglobins. These results suggest that: (1) $K_{\text{stabilization}}$ and $K_{\text{H}_2\text{O}}$ become zero when His64(E7) is replaced with an apolar amino acid, (2) the product $K_{\text{entry}}K_{\text{bond}}$ is roughly 0.01 μM^{-1} for O$_2$ binding regardless of the size of the E7 residue, and (3) the ratio $(1 + K_{\text{stabilization}})/(1 + K_{\text{H}_2\text{O}}[\text{H}_2\text{O}])$ is 100 for wild-type myoglobin, implying that the strength of the hydrogen bond to bound oxygen is considerably greater than that between His64 and non-coordinated water in deoxymyoglobin.

With the exception of the H64L mutation, only three- to fivefold increases in CO affinity are observed when His64 is replaced with apolar residues and again there is little dependence on size for the series Ala, Val, Ile, Phe. The average value of K_{CO} for 11 different apolar substitutions in pig, human, and sperm whale myoglobin is 120 ± 40 μM^{-1}, excluding the Leu64 mutants [15]. These results suggest that the water-binding term $(1 + K_{\text{H}_2\text{O}}[\text{H}_2\text{O}])$ is four times that for electrostatic stabilization $(1 + K_{\text{stabilization}})$ in wild-type CO-myoglobin. Thus, the presence of the distal histidine results in a net inhibition of CO binding.

The His64 to Ala, Val, Ile, and Phe substitutions produce little change in NO affinity (Table 1). In this case, the average value of K_{NO} is 210000 ± 60000 μM^{-1} and identical to that for the corresponding wild-type

Fig. 3 Crystal structures of wild-type MbO$_2$, wild-type MbCO, and native MbNO. Side view of the distal pocket showing hydrogen-bonding interactions as *thin yellow* and *light blue lines*. Except for the distal histidine and bound ligand, carbon, nitrogen, and oxygen atoms are *green, blue,* and *red*, respectively. The iron atom is *orange*. Atoms of the His64 side chain and the bound ligand atoms are *yellow* for MbO$_2$, *pink* for MbCO, and *cyan* for MbNO. The structures for wild-type MbO$_2$ (2mgm) and MbCO (2mgk) were taken from Quillin et al. [17]. The structure for native MbNO was taken from Brucker et al. [52] and has been deposited in the Brookhaven Protein Data Bank (lhjt)
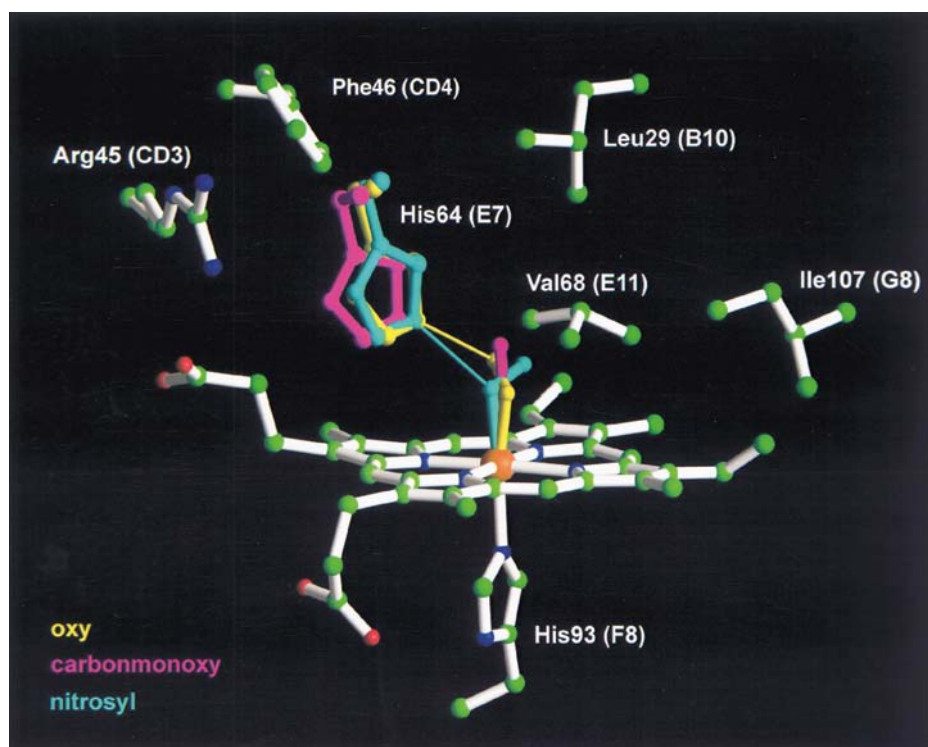

Table 2 Estimation of parameters for ligand binding to wild-type or native sperm whale deoxymyoglobin. The overall equilibrium association constant can be obtained by taking the product of the terms in the last four columns

Ligand	$\dfrac{1}{1+K_{H_2O}[H_2O]}$	K_{entry} (M^{-1})	K_{bond}	$1+K_{stabilization}$
O$_2$	0.1 ± 0.05	20 ± 10	$5 \pm 5 \times 10^2$	1000 ± 500
NO	0.1	20	1×10^{10}	10
CO	0.1	20	6×10^6	2.5

and native proteins [18][3]. This result implies strongly that the water-binding and electrostatic terms cancel {i.e. $(1+K_{stabilization})/(1+K_{H_2O}[H_2O]) \approx 1.0$ for NO binding to wild-type myoglobin}.

Leu64 myoglobin shows a tenfold higher affinity for CO than that for any of the other apolar mutants (Table 1). This abnormal increase cannot be due specifically to relief of hindrance between the linear FeCO complex and the E7 residue since the same effect is observed for NO, which has a bent geometry in the bound state (Fig. 1). The structural origin of the high affinity of the Leu64 myoglobin for NO and CO is a mystery and requires further study [17]. Abnormally high increases in CO affinity are also observed when the distal histidine in leghemoglobin is replaced with a leucine [19].

Assignment of equilibrium constants for water binding, ligand entry, bond formation, and electrostatic stabilization

Three separate observations can be used to estimate the $1/(1+K_{H_2O}[H_2O])$ term in Eq. 2. First, Gibson et al. [20, 21] have shown that the rate of NO binding to myoglobin is governed exclusively by the bimolecular rate constant for entry into the protein and can be expressed as:[4]

$$k'_{NO} = \frac{k'_{entry}}{1+K_{H_2O}[H_2O]} \qquad (3)$$

When His64 is replaced with Ala, Val, Ile, Leu, or Phe, k'_{NO} increases from 22 μM^{-1} s^{-1} to an average value of

---

[3] Eich R, Li T, Brucker EA, Ikeda-Saito M, Wilkinson AJ, Phillips GN, Olson JS, unpublished data for NO binding and the crystal structure of L29F sperm whale MbNO

[4] Equation 3 assumes that the rate of water entry is more rapid than that for the ligand. An estimate for the water equilibration time can be obtained by: (a) assuming that the bimolecular rate of water entry, $k'_{H_{2O}}$, is $\sim 2 \times 10^8$ M^{-1} s^{-1}, the value for NO binding to apolar position 64 mutants, (b) computing the value of K_{H_2O} based on the estimation that $(1+K_{H_2O}[H_2O]) \approx 10$, and (c) estimating the rate of water exit as $k_{H_2O} = K_{H_2O}/k'_{H_2O}$. The observed equilibration rate equals $\sim 2 \times 10^8$ M^{-1} s$^{-1} \cdot 55$ M $+ \sim 1 \times 10^{10}$ s^{-1} or $\sim 2 \times 10^{10}$ s^{-1}, which predicts a half-time ≈ 30–40 ps. In contrast, ligands escape the distal pocket with half-times on the order of 100 ns and enter on μs time scales [16].

190 ± 60 μM^{-1} s^{-1} with only a small dependence on the size of the residue [18][3]. This result implies that the fraction of water-free distal pockets in wild-type deoxymyoglobin, $1/(1+K_{H_2O}[H_2O])$, is ~0.1 and increases to 1 for the apolar mutants when $K_{H_2O}=0$.

Second, the overall rate of CO dissociation is determined solely by the internal rate of bond disruption [16]. Since the extent of CO recombination from the C or geminate intermediate in Fig. 2 is close to zero at room temperature, virtually all of the CO molecules that thermally dissociate from the iron atom escape to the solvent [16]. Under these conditions, the observed rate is given by:

$$k_{CO} = \frac{k_{-b}}{1+K_{stabilization}} \qquad (4)$$

The value of k_{CO} increases from 0.02 s^{-1} to 0.05 ± 0.01 s^{-1} for 11 different apolar mutations at position 64 in pig, human, and sperm whale myoglobin (excluding H64L) [15]. Since $K_{stabilization}$ should be 0 in the mutants, the increase in k_{CO} implies that $(1+K_{stabilization})$ is 2.5 for CO binding to the wild-type protein. As described in the previous section, the equilibrium constants for the same set of mutants predict that $(1+K_{stabilization})/(1+K_{H_2O}[H_2O])$ is ~0.25 for CO binding to wild-type protein. In combination, these equilibrium and kinetic results also predict that $1/(1+K_{H_2O}[H_2O])\approx0.1$ for wild-type deoxymyoglobin. Similar arguments can be applied to the effects of apolar substitutions at position 64 on the rate of O_2 dissociation. These mutations cause ~500-fold increases in k_{O_2}, indicating that $1+K_{stabilization}$ is at least 500 for FeO_2 in the wild-type protein (Table 1). However, substantial geminate recombination of O_2 occurs, and, as a result, quantitative analysis requires expansion of Eq. 4 to include terms describing the rate of internal bond formation k_b and the rate of escape from the distal pocket k_{escape} [22, 23].

Third, analyses of time courses for geminate recombination of ligands on nanosecond time scales allows an estimation of the equilibrium constant for the formation of the intermediate containing non-covalently bound ligand {i.e. $K_{entry}/(1+K_{H_2O}[H_2O])$}. In collaboration with Quentin Gibson, we have carried out seven independent determinations of this constant for native myoglobin (K_{XC} values in [21–23]). The average value is $\sim2.4\pm0.7$ M^{-1} for either O_2, CO, or NO binding at $20\,°C$ and roughly independent of the exact kinetic model used to assign rate parameters. Similar values have been reported by others [24, 25]. This parameter was also estimated for Gly64, Val64, Leu64, and Phe64 mutants of sperm whale myoglobin, and the average value was 15 ± 5 M^{-1}, with little effect of amino acid size [22]. These results also suggest that $1/(1+K_{H_2O}[H_2O])\approx0.1$ for wild-type deoxyMb and provide an estimate of $K_{entry}\approx20$ M^{-1} based on the mutant results when $K_{H_2O}=0$.

If $1/(1+K_{H_2O}[H_2O])$ is fixed at 0.1, values of $(1+K_{stabilization})$ can be calculated from the effects of apolar substitutions at position 64 on the overall equilibrium constants. Separate values of K_{bond} can be computed by assuming that K_{entry} equals ~20 M^{-1} for all three diatomic ligands. This type of analysis provides a complete set of parameters for O_2, NO, and CO binding to wild-type sperm whale myoglobin and a quantitative interpretation of the effects of polarity on ligand discrimination (Table 2).

By pulling a water molecule into the distal pocket, His64(E7) inhibits the binding of all ligands by a factor of ~10 compared to chelated protoheme dissolved in an apolar solvent. In the case of O_2 binding, this unfavorable effect is overcome by the formation of a strong hydrogen bond with the highly polar FeO_2 complex (Fig. 1). This electrostatic interaction stabilizes bound dioxygen by a factor of ~1000, and the net result is a 100-fold increase in K_{O_2} compared to simple model hemes or mutants with an apolar residue at position 64. In the case of CO binding, electrostatic interaction with His64 is very weak, resulting in only a two- to threefold stabilization of the bound ligand. The net result is a fivefold reduction in K_{CO} for the wild-type protein compared to mutants with apolar residues at position 64. In the case of NO binding, there is a tenfold stabilization of the bound ligand which exactly compensates for the tenfold inhibition due to the presence of distal pocket water. The net result is little change in K_{NO} with mutagenesis of the distal histidine. As shown in Fig. 1, the ability of FeNO to accept a proton from N of His64(E7) is expected to be intermediate between that of FeO_2, which has almost a full negative charge on the O(2) atom, and FeCO, which is a poor acceptor due to the partial triple bond character of the C–O bond.

Steric hindrance and effects of substitutions at other positions

The results in Table 1 show that the ~1000-fold reduction in K_{CO}/K_{O_2} in going from simple model hemes to myoglobin is due primarily to preferential electrostatic stabilization of bound O_2 in the protein. The strongest evidence for this conclusion is the marked 500- to 1000-fold increase in the O_2 dissociation rate constant when the distal histidine is replaced with apolar amino acids (Table 1). Intermediate results are obtained for the His64 to Gln and Gly mutations. In the case of the Gln64 mutant, hydrogen bonding to the amide side chain can still occur, although more weakly, and, in the Gly64 mutant, the open distal pocket allows partial stabilization of bound O_2 by solvent water molecules (Table 1) [17]. Thus, the protein is discriminating more in favor of O_2 binding than against CO binding.

The affinity of myoglobin for CO is reduced $\sim$ tenfold compared to that of model hemes. We have attributed most of this inhibition to the requirement of water displacement from the distal pocket {i.e. the $1/(1+K_{H_2O}[H_2O])$ term in Eq. 2 and Table 2} and not direct steric hindrance of the FeCO complex by the im-

idazole side chain of His64. The evidence for this conclusion is substantial, but not as compelling as that for O_2 stabilization. The value of K_{CO} does not appear to depend on the size of the position 64 amino acid as long as it is apolar (Table 1). The only exception is the Leu64 mutant, which shows abnormally high CO and NO affinities.

The mobility of the His64 side chain can be increased by mutating Phe46(CD4) to Val or Ala [26]. In the crystal structure of F46V aquometmyoglobin, the imidazole side chain swings between the "down" conformation shown in Figs. 1–3 and an "up" position, away from the bound ligand. His64 is predominately in the up position in the structures of the deoxy and CO forms of the mutant. As expected, these substitutions destabilize hydrogen bonding interactions with bound O_2, causing 10- to 20-fold decreases in K_{O_2} and corresponding increases in k_{O_2} (Table 1). In the steric hindrance model, enhanced mobility of His64 should relieve strain on the linear FeCO complex, causing an increase in CO affinity. The opposite effect is observed. The F46V and F46A substitutions cause two- to fourfold decreases in K_{CO}, presumably due to loss of electrostatic stabilization of the iron-carbonyl. Although not in the same location as in the wild-type protein, a water molecule attached to His64 is still present in the distal pocket of F46V deoxymyoglobin and must be displaced before ligands can bind [26]. As a result, the inhibitory $(1+K_{H_2O}[H_2O])$ term is still large, and loss of electrostatic stabilization by His64 causes decreases in affinity for all three ligands (Table 1). As predicted from the $(1+K_{stabilization})$ terms in Table 2, the biggest decrease caused by the F46V mutation is observed for K_{O_2} and the smallest for K_{CO}.

The distal valine residue is in close van der Waals contact with bound ligands in myoglobin and has been postulated to restrict linear Fe–C–O binding [Val68(E11) in Figs. 2 and 3]. Decreasing the size of this residue in sperm whale myoglobin causes a twofold increase in K_{CO} with little change in O_2 affinity. Curiously, larger differential changes occur when V68A or V68G mutations are made in human myoglobin. The M value (K_{CO}/K_{O_2}) is 170 for Ala68 human myoglobin compared to ~ 50 for the corresponding sperm whale myoglobin mutant [27][5]. Thus, steric hindrance by Val68 may be contributing a factor of 2–5 toward ligand discrimination in mammalian myoglobins. This conclusion is supported by the increase in K_{CO}/K_{O_2} from 1700 for the single H64G mutant of sperm whale myoglobin to 3200 for the H64G/V68A double mutant [28]. The V68A and H64G/V68A mutations also increase markedly the extent of geminate recombination of O_2, NO, and CO following picosecond and nanosecond laser photolysis pulses, indicating that the native Val68 residue does inhibit access of all ligands to the

iron atom [45]. Steric hindrance by residue 68 can be increased to more measurable levels by replacing the distal valine with isoleucine. As shown in Table 1, the *iso*-butyl side chain of Ile68 markedly inhibits the binding of all three ligands, the biggest effect being on CO binding [23, 28]. Again, this hindrance is observed in laser photolysis experiments in the form of lower rates and extents of geminate recombination for all three gaseous ligands [46]. Thus, as discussed by Lim et al. [47], steric hindrance does limit the rate of internal bond formation, but this effect does not appear to discriminate greatly between O_2, NO, and CO.

Two other mutants have provided strong support for the polarity mechanism. When Val68 is replaced with Thr, the β-hydroxyl of the mutant side chain forms an additional hydrogen bond with the distal pocket water molecule in deoxymyoglobin [29, Table 1]. The net effect is a significant increase in the $(1+K_{H_2O}[H_2O])$ term, which results in a decrease in affinity for all three ligands. In contrast, replacing Leu29(B10) with Phe places the positive portion of the phenyl multipole adjacent to the second bound ligand atom, preferentially enhancing O_2 and NO affinity compared to that for CO [30, Table 1]. Thus, Eq. 2 and Fig. 2 provide a useful framework for interpreting the effects of a wide range of mutations in mammalian myoglobins.

CO affinity and the Fe–C–O bond angle

One of the strongest arguments in favor of the steric hindrance mechanism for ligand discrimination is the observation of a significantly "bent" ligand geometry in $P2_1$ crystals of native MbCO, where the Fe–C–O angle is observed to be 135–150° [7, 48]. However, the structural cause of this bending is unclear and appears to be peculiar to the $P2_1$ crystal form. The observed Fe–C–O angle is $167 \pm 10°$ in P6 crystals of six different recombinant sperm whale myoglobins and almost invariant with mutations at key positions near the bound ligand [17, 23]. For example, both H64L and V68I MbCO show Fe–C–O angles equal to $\sim 165°$, even though the affinities of these mutants for CO differ by a factor of 500 (Table 1). Although the current controversy between Fe–C–O angles measured spectroscopically and those determined by crystallography remains unresolved [47–49], this problem appears to be less important than originally thought since CO affinity cannot be predicted by this angle. This latter view is supported by recent theoretical calculations which indicate that the free energy required for bending FeCO is not as great as originally thought [50, 51].

Proximal effects and applications to other reversible O_2-binding proteins

Although we have focused on distal residues, the reactivity of the heme iron atom can be altered to an even

---

[5] Li T, Dou Y, Ikeda-Saito M, Olson JS, unpublished data comparing position 68 mutations in human, pig, and sperm whale myoglobin

Table 3 Comparison of the ligand affinities of sperm whale myoglobin, soybean leghemoglobin a, R-state human hemoglobin and T-state human hemoglobin

Protein	K_{O_2} μM^{-1}	k_{O_2} s^{-1}	K_{CO} μM^{-1}	K_{NO} μM^{-1}
Sperm whale myoglobin	1.1	15	27	220000
Soybean leghemoglobin a[a]	23	5.6	2000	9000000
R-state Human Hb[b]	2.4	15–35	750	5000000
T-state Human Hb (inositol-P_6)[b]	0.003	2000–4000	0.5	5000

[a] Data were taken from Hargrove et al. [19] and are for recombinant Lba expressed in *E. coli*
[b] The rate constants for O_2 and CO binding were taken from unpublished work with metal hybrids of human hemoglobin by Unzai S, Eich RF, Shibayama N, Olson JS, and Morimoto H from Rice and Osaka Universities. The R-state were parameters computed as the average of the α(ferrous) and β(ferrous) rate constants for Mn(III)/Fe(II) and Cr(III)/Fe(II) hybrids at pH 8.4; the T-state parameters were computed as the average of the α(ferrous) and β(ferrous) rate constants for Mg(II)/Fe(II) and Ni(II)/Fe(II) hybrids at pH 6.5 in the presence inositol hexaphosphate to ensure complete conversion to the low-affinity quaternary conformation. The parameters for NO binding to hemoglobin were calculated from the ratio of measured association and dissociation rate constants. For the R-state, the average value of k'_{NO} for both isolated α and β subunits and those in tetramers is ~ 50 μM^{-1} s^{-1} (Mathews AJ, Aitken JF, Lemon DD, Olson JS, unpublished data) and that for k_{NO} is $\sim 1 \times 10^{-5}$ s^{-1} [42]. For the T-state, Gibson and Cassoly [43] reported a value of $k'_{NO} = 30$ μM^{-1} s^{-1}, and Hille and Olson [44] reported that $k_{NO} \approx 6 \times 10^{-3}$ s^{-1} for single-ligand hemoglobin at pH 6.5 in the presence of inositol hexaphosphate

greater extent by geometrical or chemical constraints on the proximal side of the heme group. Two of the best known examples of these effects are shown in Table 3. Soybean leghemoglobin shows 20, 70, and 40 times higher affinities for O_2, CO, and NO, respectively, than sperm whale myoglobin. This increase in reactivity has been ascribed to greater mobility of the proximal His(F8) residue, which facilitates in-plane movement of the iron and formation of strong hexacoordinate complexes with all ligands [31]. Some discrimination between the ligands appears to occur since the increase in O_2 affinity is ~ 3 times less than the increase in CO affinity. However, Hargrove et al. [19] have shown that the distal histidine in leghemoglobin does not appear to form a strong hydrogen bond with the FeO_2 complex at neutral pH. Thus, the differences between the M values for sperm whale myoglobin and leghemoglobin can be explained by the differences in the $(1 + K_{stabilization})$ term in Eq. 2, even though K_{bond} is much greater in the plant protein.

Even larger changes in ligand affinity are observed when comparing equilibrium constants for ligand binding to the R and T states of human hemoglobin. In this case, the α and β heme pockets contain the same amino acids, and the quaternary changes primarily cause movements of the F and E helices, which restrict the ability of the iron atom to move into the plane of the porphyrin ring and react with ligands [32, 33]. As shown in Table 3, the R to T transition causes 700-, 1500-, and 1000-fold decreases in K_{O_2}, K_{CO}, and K_{NO}, respectively. As in the case of leghemoglobin, the higher K_{CO}/K_{O_2} ratios observed for human hemoglobin have been shown to be due to a significantly weaker hydrogen-bonding interaction between the distal histidine and bound O_2 than that observed in myoglobin [34].

Conclusions

The affinity of myoglobins and hemoglobins for ligands can be varied over several orders of magnitude by either distal or proximal protein interactions. However, the key factor regulating discrimination between O_2, CO, and NO binding involves electrostatic interactions with the bound ligand and solvent water molecules on the distal side of the heme group. Residues with good hydrogen atom donors (i.e. His, Gln) favor the binding of dioxygen by preferentially stabilizing the highly polar $Fe^{\delta(+)}-O-O^{\delta(-)}$ complex. At the same time, these residues often bring a water molecule into the protein, which must be displaced before ligands can bind. The presence of a distal-pocket water molecule causes a net inhibition of CO binding, since little electrostatic stabilization can occur for the neutral FeCO complex. The FeNO complex shows intermediate behavior, the favorable electrostatic interaction being roughly equal to the inhibitory effect of water binding in native or wild-type deoxymyoglobin. These effects can be quantified by assigning values to the equilibrium constants for non-covalent water binding to deoxymyoglobin, ligand entry into the distal pocket, internal coordination to the iron atom, and electrostatic stabilization of the bound ligand. The resulting set of parameters and the corresponding expression for the overall equilibrium association constant (Eq. 2) provide a useful framework for both interpreting and predicting the ligand-binding behavior of a wide range of myoglobins and hemoglobins.

552

References

1. Brantley RE, Smerdon SJ, Wilkinson AJ, Singleton EW, Olson JS (1993) J Biol Chem 268:6995–7010
2. Marks GS, Brien JF, Makastu K, McLaughlin BE (1991) Trends Pharmacol Sci 121:185–188
3. Verma A, Hirsch DJ, Glatt CE, Ronnett GV, Snyder SH (1993) Science 259:5681–5684
4. Morita TA, Perrella MA, Lee ME, Kourembanas S (1995) Proc Natl Acad Sci USA 92:1475–1479
5. Collman JP, Brauman JI, Halber TR, Suslick KE (1976) Proc Natl Acad Sci USA 73:333–3337
6. Collman JP (1977) Acc Chem Res 10:265–272
7. Kuriyan J, Eilz S, Karplus M, Petsko GA (1986) J Mol Biol 192:133–154
8. Jameson GB, Ibers JA, (1994) In: Betini I, Gray HB, Lippard SJ, Valentine JS (eds) BioInorganic Chemistry. University Books, Sausalito, Calif, USA
9. Weiss JJ (1964) Nature 202:83–84
10. Momenteau M, Reed CA (1994) Chem Rev 94:659–698
11. Traylor TG, White DK, Campbell DH, Berzinis AP (1981) J Am Chem Soc 103:4932–4936
12. Traylor TG, Mitchell M, Tsuchiya S, Campbel DH, Stynes DV, Koga, N (1981) J Am Chem Soc 103:5234–5236
13. Traylor TG, Koga N, Deardruff LA (1985) J Am Chem Soc 107:6504–6510
14. Olson JS, McKinnie RE, Mims MP, White DK (1983) J Am Chem Soc 105:1522–1527
15. Springer BA, Sligar SG, Olson JS, Phillips GN (1994) Chem Rev 94:699–714
16. Olson JS, Phillips GN (1996) J Biol Chem 271:17593–17596
17. Quillin ML, Arduini RM, Olson JS, Phillips GN (1993) J Mol Biol 234:140–155
18. Eich RF, Li T, Lemon DD, Doherty DH, Curry SR, Aitken JF, Mathews AJ, Johnson KA, Smith RD, Phillips GN, Olson JS (1996) Biochemistry 35:6976–6983; Eich RF (1997) PhD dissertation, Rice University
19. Hargrove MS, Barry JK, Brucker EA, Berry MB, Phillips GN, Arrendondo-Peter R, Dean JM, Klucas RV, Sarath G (1997) J Mol Biol 266:1032–1042
20. Gibson QH, Olson JS, McKinnie RE, Rohlfs RJ (1986) Biol Chem 261:10228–10239
21. Gibson QH, Regan R, Elber R, Olson JS, Carver TE (1992) J Biol Chem 267:22022–22034
22. Carver TE, Rohlfs RJ, Olson JS, Gibson QH, Blackmore RS, Springer BA, Sligar SG (1990) J Biol Chem 265:20007–20020
23. Quillin ML, Li T, Olson JS, Phillips GN, Dou Y, Ikeda-Saito M, Elber R, Li H, Regan R, Gibson QH (1995) J Mol Biol 245:416–436
24. Henry ER, Sommer JH, Hofrichter J, Eaton WA (1983) J Mol Biol 166:443–451
25. Jongeward KA, Magde D, Taube DJ, Marsters JC, Traylor TG, Sharma VS (1988) J Am Chem Soc 110:380–387
26. Lai HH, Li T, Lyons DS, Phillips GN, Olson JS, Gibson QH (1995) Proteins: Struct Function Genet 22:322–339
27. Lambright DG, Balasubramanian S, Decatur S, Boxer SG (1994) Biochemistry 33:5518–5525
28. Egeberg KD, Springer BA, Sligar SG, Carver TE, Rohlfs RJ, Olson JS (1990) J Biol Chem 265:11788–11795
29. Smerdon SJ, Dodson GG, Wilkinson AJ, Gibson QH, Blackmore RS, Carver TE, Olson JS (1991) Biochemistry 30:6252–6260
30. Carver TE, Brantley RE, Singleton EW, Arduini RM, Quillin ML, Phillips GN, Olson JS (1992) J Biol Chem 267:14443–14450
31. Harutyunan EH, Safonova TN, Kuranova IP, Popov AN, Teplyakov AV, Obmolova GV, Rusakov AA, Vainshtein BK, Dodson GG, Wilson JC, Perutz MF (1995) J Mol Biol 251:104–115
32. Perutz MF, Fermi G, Luisi B, Shaanan B, Liddington RC (1987) Ass Chem Res 20:309–321
33. Perutz MF (1990) Annu Rev Physiol 52:1–25
34. Mathews AJ, Rohlfs RJ, Olson JS, Tame J, Renaud JP, Nagai K (1989) Biol Chem 264:16573–16583
35. Maxwell JC, Caughey WS (1976) Biochemistry 15:388–396
36. Sampath V, Zhao XJ, Caughey WS (1994) Biochem Biophys Res Commun 198:281–287
38. Li T, Quillin ML, Phillips GN, Olson JS (1994) Biochemistry 33:1433–1446
39. Ling J, Li T, Olson JS, Bocian DF (1994) Biochim Biophys Acta 1188:417–421
39. Ray GB, Li XY, Ibers JA, Sessler JL, Spiro TG (1994) J Am Chem Soc 116:162–176
40. Benko B, Yu NT (1983) Proc Natl Acad Sci USA 80:7042–7046
41. Scheidt WR (1977) Acc Chem Res 10:339–345
42. Hirota S, Li T, Phillips GN, Olson JS, Mukai M, Kitagawa T (1996) J Amer Chem Soc 118:7845–7846
42. Moore EG, Gibson QH (1976) J Biol Chem 251:2788–2794
43. Cassoly R, Gibson QH (1975) J Mol Biol 91:301–313
44. Hille CR, Olson JS, Palmer GA (1979) J Biol Chem 254:12110–12120
45. Carlson M, Regan R, Elber R, Li H, Philips GN, Olson JS, Gibson QH (1994) Biochemistry 33:10597–10606
46. Ikeda-Saito M, Dou Y, Yonetani T, Olson JS, Li T, Regan R, Gibson QH (1993) J Biol Chem 268:6855–6857
47. Lim M, Jackson TA, Anfinrud PA (1997) J Biol Inorg Chem (in press)
48. Sage TL (1997) J Biol Inorg Chem (in press)
49. Slebodnick C, Ibers JA (1997) J Biol Inorg Chem (in press)
50. Vangberg T, Bocian DF, Ghosh A (1997) J Biol Inorg Chem (in press)
51. Spiro TG, Kozlowski DM (1997) J Biol Inorg Chem (in press)
52. Brucker EA, Olson JS, Ikeda-Saito M, Phillips GN (1997) Biochemistry (submitted)